Supplementary Material

NiFe Alloy Nanocrystals Anchored on Nitrogen-Doped Carbon: Interface Engineering for Enhanced Peroxymonosulfate Activation via Non-Radical Dominanted Pathway

Xiaoqin Sun,*[a] Meiluo Jiang [a], Hao Chen [a], Hongmei Chen[e] and Xiaoxiang Xu *[b,c,d]

[a]*School of Chemistry and Chemical Engineering, Xi'an University of Architecture and Technology, Xi'an 710055, Shaanxi, China.*
E-mail: sunxiaoqin@xauat.edu.cn

[b]*Department of Neurosurgery, Tongji Hospital, Tongji University School of Medicine, Tongji University, Shanghai, 200065, P. R. China. E-mail: xxxu@tongji.edu.cn*
[c]*Clinical and Central Lab, Putuo People's Hospital, Tongji University, Shanghai, 200060, P. R. China*

[d]*Shanghai Key Lab of Chemical Assessment and Sustainability, School of Chemical Science and Engineering, Tongji University, Shanghai, China.*

[e]*Wenzhou Key Laboratory of Novel Optoelectronic and Nanomaterials, Institute of Wenzhou, Zhejiang University, 26 Fengnan Road, Wenzhou 325006, China.*

Text S1

The detailed information of chemicals used in this study.

Iron nitrate nonahydrate ($Fe(NO_3)_3·9H_2O$, 98%) and Cobalt nitrate hexahydrate (($Ni(NO_3)_2·6H_2O$, 99%) was purchased by Sinopharm Group Chemical reagent Co., LTD. Polyaniline (PANI) was bought from Shanghai Macklin Biochemical Technology Co., LTD. Potassium peroxymonosulfate (PMS) was bought from Shanghai Aladdin Biochemical Technology Co., LTD. P-Ben-zoquinone (p-BQ) was supplied by Tianjin Dean Chemical Reagent Co., LTD. Sodium chlorid (NaCl), sodium nitrate ($NaNO_3$), sodium bicar-bonate ($NaHCO_3$), sodium dihydrogen phosphate (Na_2HPO_4) and humic acid (HA) were purchased from Tianli Chemical Reagents Co., LTD.

Text S2

Characterization

The X-ray diffraction (XRD) pattern was provided by a Bruker D8 focus diffractometer with Cu Kα X radiation (45 kV, 100 mA) to determine the composition and purity of the catalysts. The surface morphologies were measured by a field emission scanning electron microscope (SEM, Gemini 500) equipped with energy dispersive spectroscopy (EDS, UltimMax100). The microstructure, crystal structure, and elemental distribution of the as-prepared heterogeneous catalyst were characterized using a Transmission Electron Microscope (TEM, JEOL JEM-F200). Fourier transform infrared (FTIR) spectra were recorded on Thermo Scientific Nicolet spectrophotometer (iS50). Raman spectra were collected on the LabRAM HR Evolution. X-ray photoelectron spectroscopy (XPS, Thermo Scientific Escalab 250Xi) was used to measure the surface chemical properties. All the binding energies were calibrated by the C 1s peak centered at 284.8 eV. The N_2 adsorption-desorption isotherms of the samples were measured using a Micromeritics ASAP 3020 analyzer. The specific surface area was then determined by applying the Brunauer-Emmett-Teller (BET) method to the corresponding data. The concentration of Fe and Ni leached from catalysts was measured by an inductively coupled plasma emission spectrometer (ICP, Shimadzu, Japan). Thermogravimetric analysis (TGA) was performed using a thermogravimetric analyzer (Rigaku, Japan) to investigate the relationship between the catalyst's mass and temperature, thereby analyzing the mass change of the N-C content before and after heat treatment. The measurement was conducted under a N_2 atmosphere with a target temperature of 800 °C and a heating rate of 5 °C/min. The solutions sampled at reaction times of 20, 60, and 120 minutes were first filtered through a 0.22 μm membrane filter and then analyzed using a Total Organic Carbon analyzer (TOC-L CPH, SHIMADZU, Japan).

Electrochemical test was carried out on electrochemical workstation (CHI660D, Shanghai Chenhua Instrument Co., LTD.) equipped with a standard three-electrode system. The prepared catalyst was uniformly dispersed in naphthol solution and coated on the FTO electrode as a working electrode. Meanwhile, a platinum sheet was used as the counter electrode, and a saturated calomel electrode (SCE) was employed as the reference electrode.

Text S3

Experimental procedure

The catalytic performance of the catalysts was evaluated by means of the degradation of TC. In a typical experiment, a 250 mL beaker was equipped with 200 mL of TC solution at a concentration of 10 mg/L, and the catalysts were used for the catalytic performance evaluation. At the commencement of the experiment, 20 mg of NiFe@N-C and 1 mM of PMS were added to the solution. To study the effect of different activator species on the catalytic system, the concentration of the activator was 1 mM. To study the effect of initial pH on the catalytic experiments, the TC solution was pH adjusted by using a 0.1 M solution of HCl and a 0.1 M solution of NaOH. To determine the pH value during the reaction process, we withdrew 1 mL of solution every 10 minutes and measured the pH using a pH meter under precise conditions. For the experiment of different anions present in the water column, $NaNO_3$, NaCl and $NaHCO_3$ were added to the solution at a concentration of 1 mM. The concentration of HA was 10 mg/L. Quenching experiments were carried out with methanol (MeOH), p-benzoquinone (PBQ), and furfuryl alcohol (FFA) as the quencher, respectively. Dimethyl sulfoxide (DMSO) was added at concentrations of 1 mM, 5 mM, and 10 mM, respectively, as a quencher for high-valent metal-oxo species. To evaluate cycling performance, the reaction solution was centrifuged after 60 minutes to obtain the spent catalyst, which was then added to a freshly prepared TC solution to continue degradation. At 10-minute intervals, 3.2 mL of the solution was filtered through a 0.22-micrometre membrane, and the concentration of TC was analyzed by ultraviolet-visible spectroscopy (UV-6100PCS, Shanghai) based on the maximum change in absorption at 355 nanometers.

Text S4

Analytical methods

The absorbance analyzed by UV-visible spectrophotometer (UV-6100pcs, Mapadainstrum Co. Ltd.) responds to the concentration of TC according to the Lambert-Beer law. The degradation efficiency corresponding to time can be calculated by Eq. (S1).

$$\text{Degradation efficiency (\%)} = \frac{c_0 - c_t}{c_0} \times 100\% \quad \text{（S1）}$$

Where C_0 and C_t are used to denote the concentration of the TC solution at 0 min and t min, respectively.

The concentration of PMS was determined by the KI colorimetric method[1]. Specifically, 100 uL degradation solution was added to 10 ml KI buffer solution contained 0.05 g $NaHCO_3$ and 0.40g KI. After the reaction for 5 minutes, the solution was measured at 352 nm by UV-VIS spectrophotometer. PMS utilization efficiency was calculated by Eq. (S2)

$$PMS\ Utilization\ Efficiency\ (\%) = \frac{[PMS]_0 - [PMS]_t}{[PMS]_0} \times 100\% \quad (S2)$$

Where $[PMS]_0$ and $[PMS]_0$ represent the initial PMS concentration (at 0 min) and the residual PMS concentration at reaction time t, respectively.

ROS was directly analyzed by Electron paramagnetic resonance (EPR, Bruker EMXmicro-6/1, Germany) with 5,5-dimethyl-1-pyrroline N-oxide (DMPO) and 2,2,6,6-Tetramethylpiperidinooxy (TEMP) as spin trapping agents. The intermediates of degradation process were identified by Liquid Chromatograph-Mass Spectrometer (LC-MS, Ultimate 3000, Thermo Scientific Q Exactive).

LC-MS was used to identify the intermediates of TC degradation. LC (Dinonex Ultimate 3000 UHPLC) is equipped with an Eclipse Plus C18 column (100mmx4.6mm, 3.5 μm). Solution A contained 0.1% formic acid in water and solution B is methanol. The ratios of solution A to B in mobile phases A and B were (10:90) and (80:20), respectively. The total flow rate was 0.4 mL/min with gradient elution. The column temperature was set to 30 ◦C. The MS (Thermo Scientific Q Exactive) conditions were electrospray ionization mode positive, probe temperature 320 ◦C, capillary voltages 3.8 kV, flow rate of nitrogen 15 L/min and full scan 50-600 m/z.

The toxicity of TC and its degradation intermediates was assessed using the Toxicity Estimation Software Tool (T.E.S.T.), with evaluations conducted for the following endpoints: Fathead minnow LC50, Daphnia magna LC50, Developmental toxicity, and Mutagenicity.

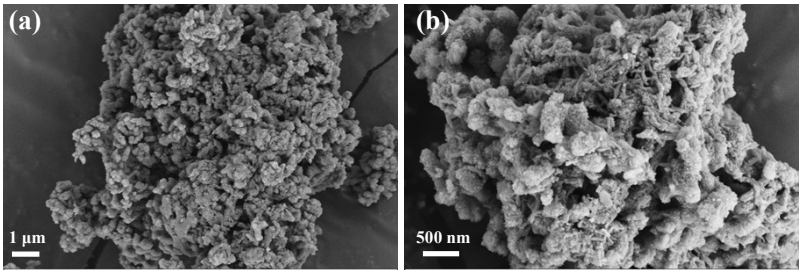

Fig. S1. SEM images of PANI

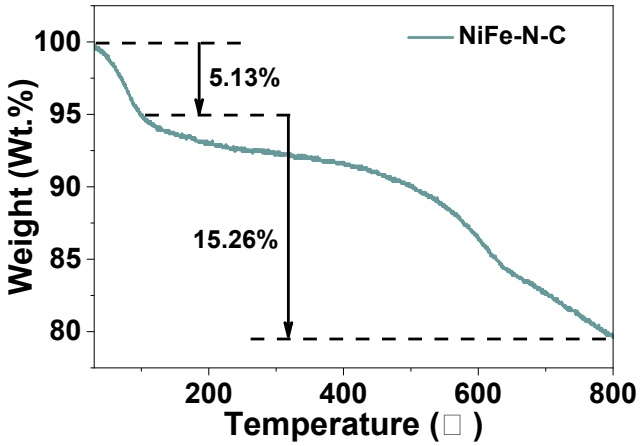

Fig. S2. TGA curve of NiFe-N-C

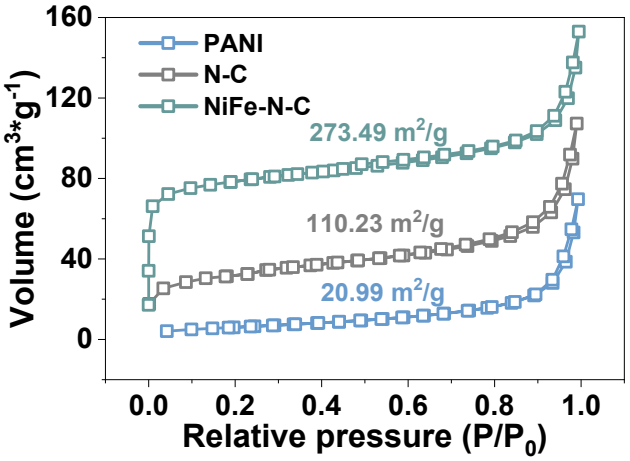

Fig. S3. N_2 adsorption-desorption isotherms

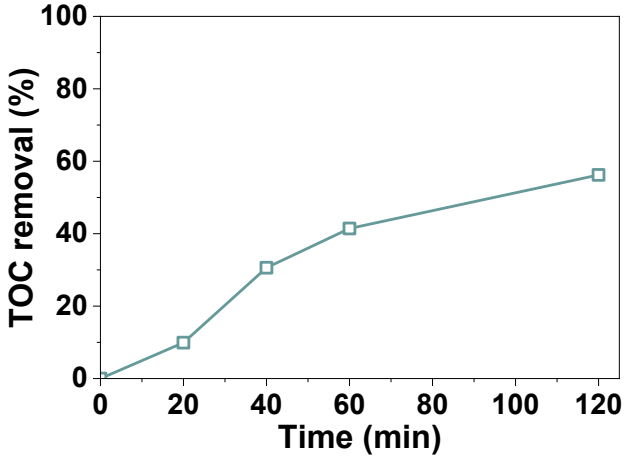

Fig. S4. TOC removal during TC degradation in the NiFe-N-C/PMS system

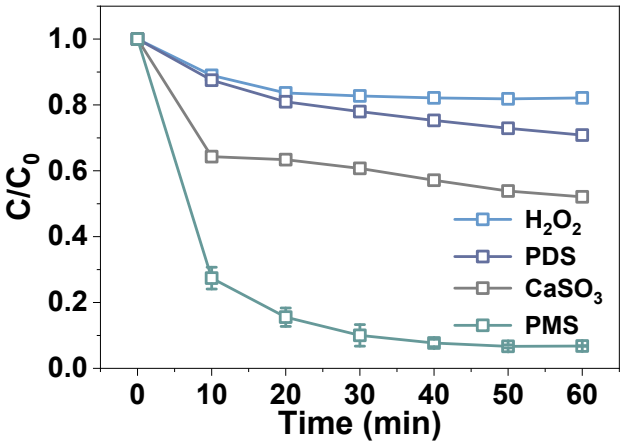

Fig. S5. Activation of various oxidants over the NiFe-N-C catalyst

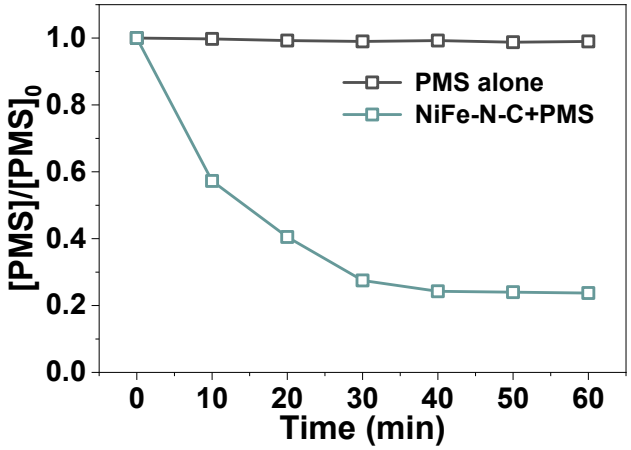

Fig. S6. PMS utilization in different systems.

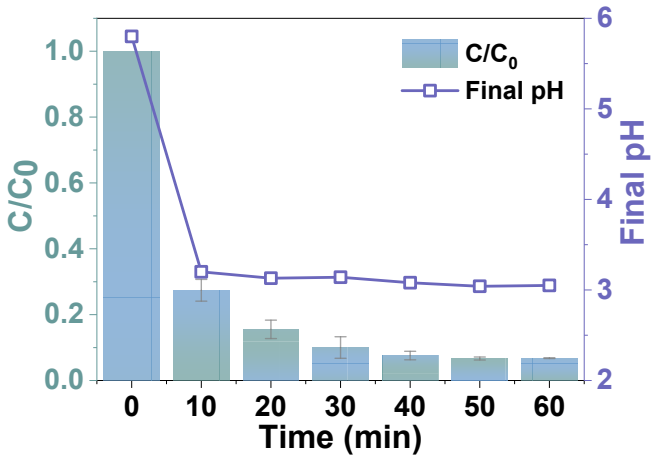

Fig. S7. TC degradation and pH variation in the NiFe-N-C/PMS system

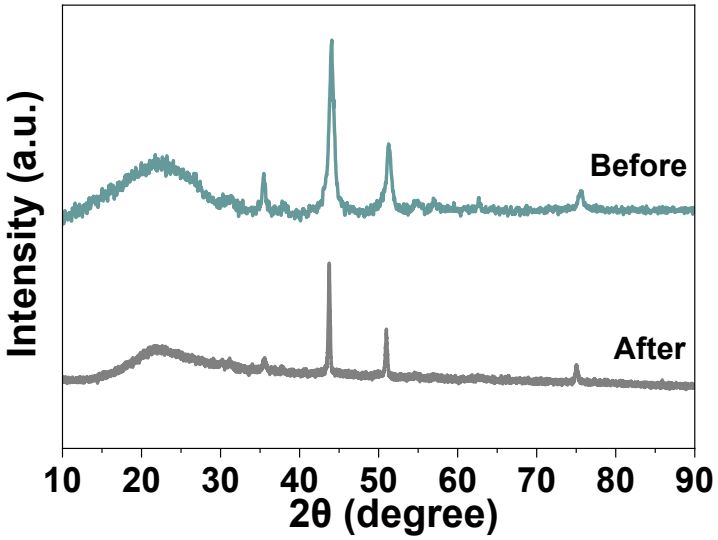

Fig. S8. XRD patterns of the NiFe-N-C catalyst before and after the reaction

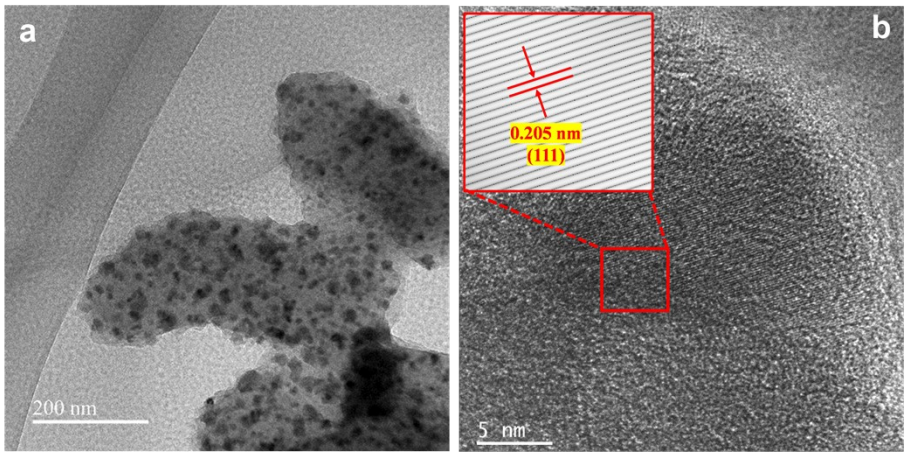

Fig. S9. (a) TEM and (b) HRTEM image of the NiFe-N-C catalyst after the reaction

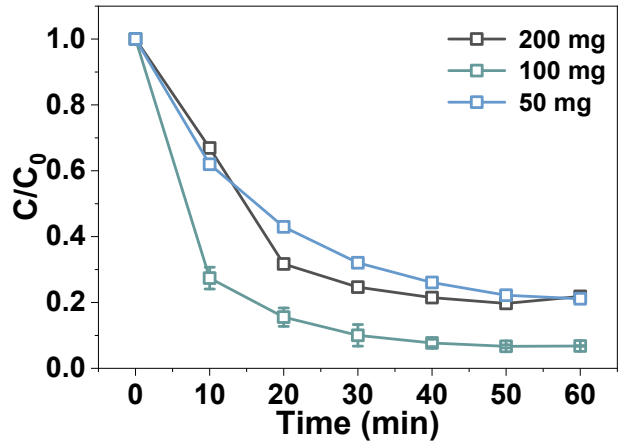

Fig. S10. Effect of PANI addition on TC degradation in NiFe-N-C/PMS catalytic system.

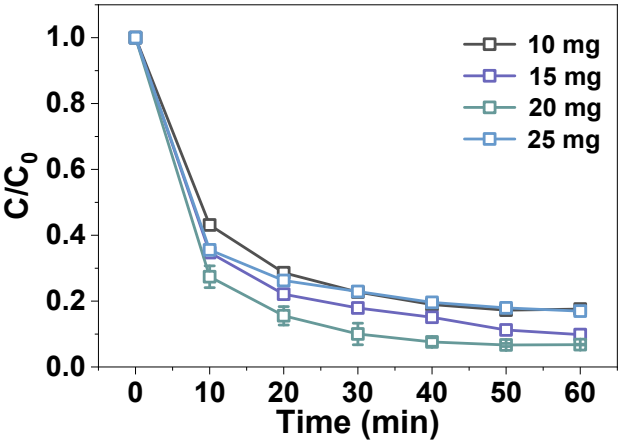

Fig. S11. Effect of NiFe-N-C dosage on TC degradation in NiFe-N-C/PMS catalytic system

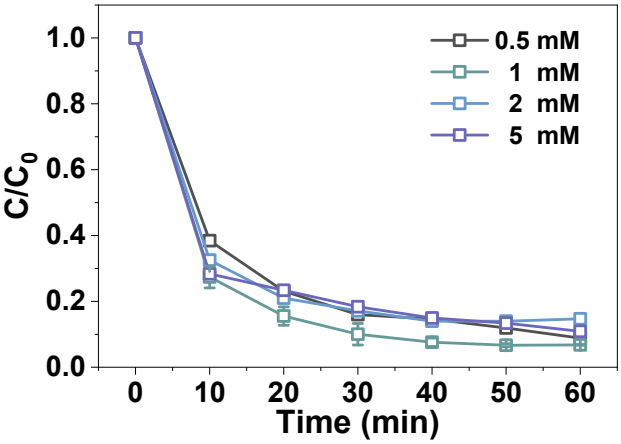

Fig. S12. Effect of the concentration of PMS on TC degradation in NiFe-N-C/PMS catalytic system

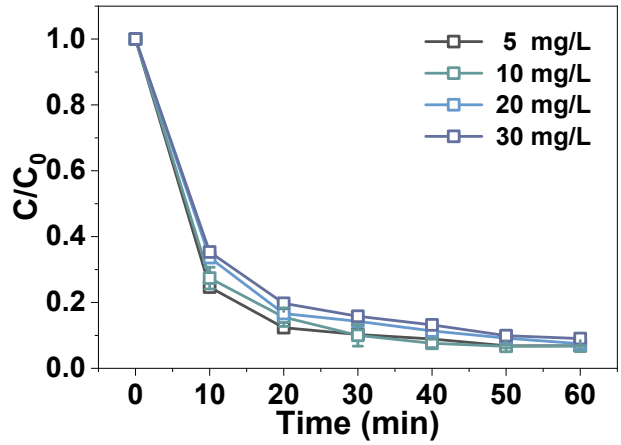

Fig. S13. Effect of TC concentrations on TC degradation in NiFe-N-C/PMS catalytic system

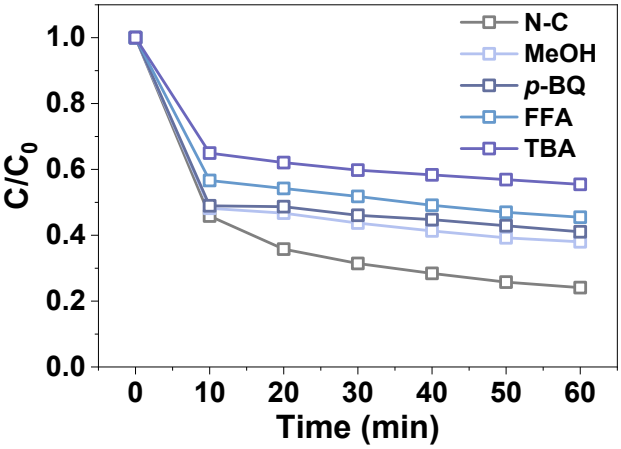

Fig. S14. TC degradation with different kinds of scavengers in N-C/PMS system

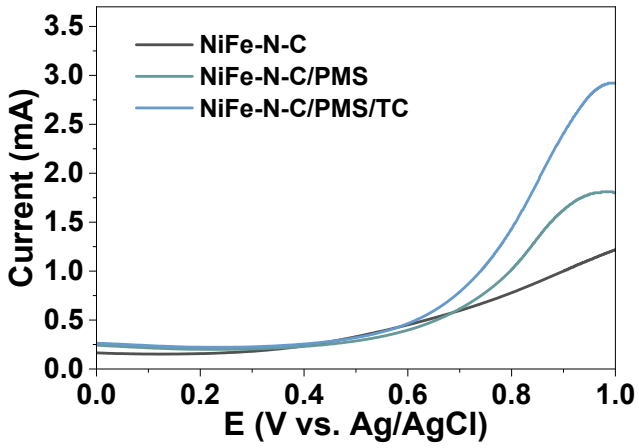

Fig. S15. LSV curves in different systems

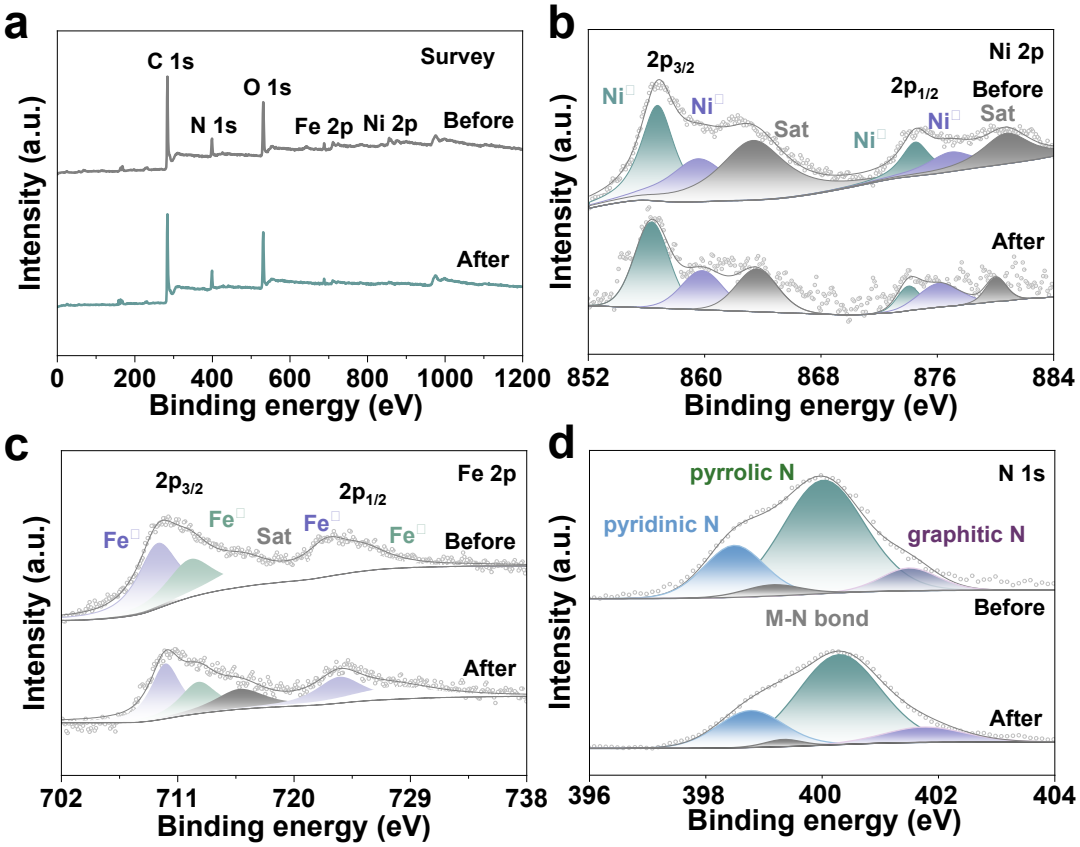

Fig. S16. XPS spectra: (a) Survey scan; (b) Ni 2p, (c) Fe 2p and (d) N 1s spectra of NiFe-N-C before and after reaction

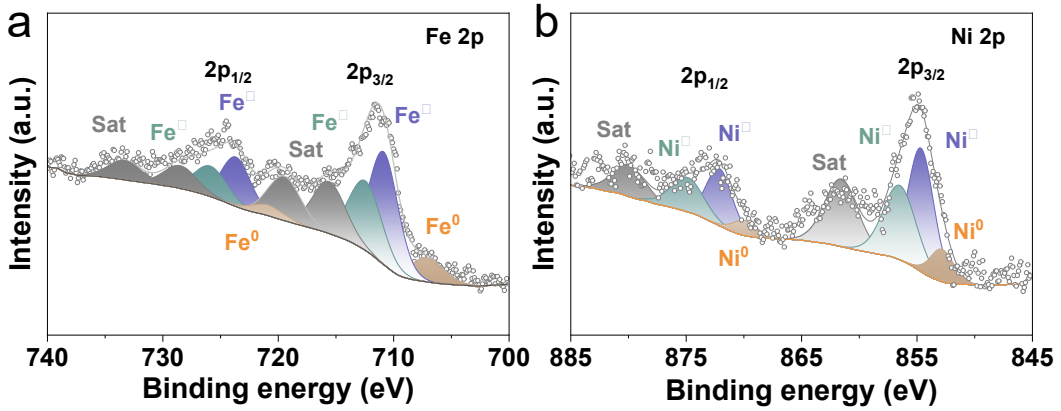

Fig. S17. XPS spectra of NiFe-N-C after etching treatment: (a) Fe 2p, (b) Ni 2p

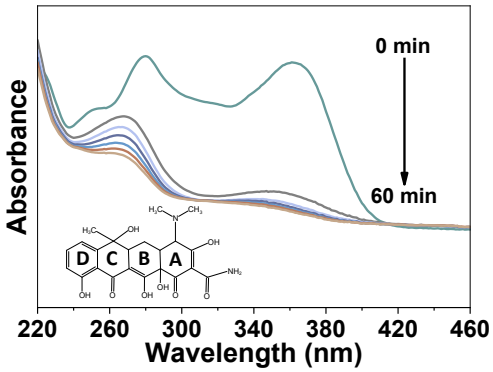

Fig. S18. UV-visible absorption spectra of TC during the degradation process

Table S1. Comparison of the PMS activation in different system

Catalyst (g/L)	PMS (mM)	Pollutant (mg/L)	pH	t (min)	UE_{PMS} %	Efficiency (%)	Ref.
NiFe-N-C (0.1)	**1**	**TC (10)**	**5.8**	**60**	**79.8**	**93.3**	**This work**
Fe-NC (5)	1.6	TC (30)	5.0	30	53.0	94.0	[2]
$CuFe_2O_4$ (0.4)	0.5	Sulfamethoxazole (5)	4.0	60	46.1	51.8	[3]
Fe_2O_3 (0.4)	3.3	Bisphenol A (50)	6.72	60	29.2	54.7	[4]
CuO (0.4)	3.3	Bisphenol A (50)	6.72	60	9.1	26.1	[4]
rGO (1.77)	0.35	Ranitidine (5)	6.0	30	46.5	91.5	[5]
E/rGO (1.77)	0.35	Ranitidine (5)	6.0	30	57.4	97.0	[5]
Mn_2O_3-D (0.1)	0.1	Bisphenol A (10)	7.0	15	54.3	88.4	[6]
N-sZVI@NC (0.3)	0.3	Ciprofloxacin (30)	6.0	30	48.4	97.3	[7]
B-nZVI (0.05)	0.1	Sulfamethoxazole (10 μM)	initial	40	71.4	79.0	[8]
N-nZVI (0.05)	0.1	Sulfamethoxazole (10 μM)	initial	40	63.1	49.0	[8]
Fe^0 (0.75)	0.26	Bisphenol A (10)	initial	40	25.0	75.2	[9]
NG (0.1)	0.25	Phenol (0.1 mM)	4.0	60	-	<60%	[10]
$CoSe_2$ (0.4)	2.0	Sulfadiazine (30)	7.0	30	70.8	100	[11]
NiFe-1 (0.8)	30mg	Tetracycline hydrochloride (20)	4.7	60	-	91.8	[12]

Reference

1. A. Jawad, K. Zhan, H. B. Wang, A. Shahzad, Z. H. Zeng, J. Wang, X. Q. Zhou, H. Ullah, Z. L. Chen and Z. Q. Chen, Environ. Sci. Technol., 2020, 54, 2476-2488.
2. Y. X. Zou, S. H. Fu, Z. Y. Xu, X. C. Zhou, J. Li, Y. Y. Zhang, Y. Lu, S. Y. Li and T. T.

Zhang, Chem. Eng. J., 2025, 505, 159684.
3. Y. Li, J. Ren, J. Ding, Y. Wang, H. Yan, F. Liu, J. Wei, X. Zhai, A. Al-Anazi and P. Falaras, J. Hazard. Mater., 2025, 488, 137312.
4. Y. Xu, J. Ai and H. Zhang, J. Hazard. Mater., 2016, 309, 87-96.
5. Y. Zhang and Z. Zhang, Chem Catal., 2024, 4, 101056.
6. X. L. Zhang, Q. Zhao, H. H. He, C. Y. Zhang, L. L. Zhao and B. N. Li, Environ. Res., 2025, 264, 120409.
7. K. Yuan, D. Chen, S. Ma, G. Du, H. Ding, F. Li and Y. Zhu, Adv. Funct. Mater., 2025, e28553.
8. W. Xu, D. Huang, Z. Wei, G. Wang, L. Du, W. Zhou, H. Huang, Y. Lei and H. Chen, Appl. Catal. B Environ. Energy, 2026, 385, 126280.
9. Y. Deng, X. Wang, P. Ning, I. Lynch, Z. Guo, P. Zhang and L. Wu, Chem. Eng. J., 2025, 523, 168772.
10. Z. Yao, Y. Chen, X. Wang, K. Hu, S. Ren, J. Zhang, Z. Song, N. Ren and X. Duan, Nat. Commun., 2025, 16, 148.
11. Y. Huang, K. Zhu, Z. Hu, Y. Chen, X. Li, Z. Jiang, M. Sillanpää, J. Zhao, R. Qiu and K. Yan, J. Hazard. Mater., 2024, 466, 133611.
12. L. Luo, K. Huang, S. Wang, Y. Wang, L. Wang and X. Liu, J. Environ. Chem. Eng., 2025, 13, 119679.
13. X. Chen, T. Guo, L. Yin, Y. Zhang, J. Niu and J. C. Crittenden, Chem. Eng. J., 2023, 471, 144774.